THERMAL MANAGEMENT ISSUES FOR MULTIFUNCTIONAL SOLAR ARRAYS

J.A. Foster and G.S. Aglietti
School of Engineering Sciences, University of Southampton
Highfield, Southampton, Hampshire, SO16 1BJ
United Kingdom

1. ABSTRACT

The structure of a satellite is critical in ensuring that a functional spacecraft reaches its destination and maintains its specified configuration. The concept of multifunctional structures has been developed to optimise the functionality of spacecraft by avoiding structural redundancies. This is done by using advances in electronics and materials to create structural elements that perform other subsystem functions. The removal of parasitic structures results in a satellite that is both cheaper to launch and more efficient during its mission.

The specific application of multifunctional structure technology addressed in this paper is the inclusion of batteries into the structure of a solar array. This removes the support structure required for the batteries and power conditioning units and reduces the wiring and volume requirements of the satellite. The major issue that is preventing the practical implementation of this concept is the tight thermal operating constraints of the batteries.

A simple version of a multifunctional solar array is proposed using a commercially available lithium polymer battery and is thermally modelled in a steady state analysis to determine the extent of the problem. It is found that thermal control is required. Three potential solutions involving the use of insulating material are modelled and found to be insufficient in a steady state model. Thermal control methods, assessed by transient analysis that could be used to solve the problem are identified.

2. INTRODUCTION

Multifunctional Structures (MFS) are defined as those components that fulfil one or more functions in addition to a structural function.

2.1. Benefits of Multifunctional Structures

The driving need behind MFS is to increase the efficiency of spacecraft as more efficient spacecraft provide better value and have better mission performance. This is a design driver as more efficient spacecraft allow more organisations to use spacecraft to further their enterprises. With an improvement in individual spacecraft efficiency, constellations of spacecraft become within the reach of more organisations [1]. The efficiency of spacecraft is improved by decreasing the mass and volume of the spacecraft and by reducing the design time and manual labour required to design and manufacture the spacecraft.

Mass is saved in a design using MFS through the incorporation of materials and components into the MFS and the removal of the supporting parasitic structure and harness used to attach the subsystem components into the spacecraft. As launch costs are directly linked to the mass of the spacecraft, a lower mass gives lower launch costs. The reduction in mass reduces the loads placed on the structure during launch which allows for a further mass decrease of the structure.

By moving the subsystem components into an MFS and removing the supporting items, a reduced volume is required inside the spacecraft. This allows the spacecraft to be smaller thus reducing the mass and the associated launch costs.

Significant touch labour is required in the assembly of traditionally designed spacecraft, a large aspect of which is the mounting of components into their frames and the connection of the wiring harness. The modular nature of an MFS would remove the need for separate component installation and reduce the risk of errors in integration.

MFS can be used in a modular design strategy but it is limited by the need to customise most aspects of a MFS to the spacecraft in question.

MFS performs better than the current light weighting strategies used to scale larger spacecraft down into the small satellite class [2]. The reduction in required volume and mass from repackaging and miniaturisation of components is limited by the need for a separate box for each separate component and thus cannot achieve the same efficiency as MFS.

2.2. Risks of Multifunctional Structures

The risks of MFS come during the design and assembly and could deny the economical advantages.

The nature of MFS, in that it combines subsystems, requires that the design teams work very closely with each other as they are effectively designing one product. If communication breaks down then the design process will be slowed and costs will be incurred. A concurrent engineering approach will improve communication and speed up the design process but will incur start up costs [3].

MFS involves advanced technology being brought together in new ways. This leads to an increase in complexity and the level of understanding required by the designers. This makes it more likely that design fault will occur in an environment where design faults will have a greater effect on the associated products due to increased component interaction. It will also require training for the designers and slow the design process.

Errors and damages during the assembly will be harder to repair as MFS are typically assembled using permanent methods (for example epoxy glues). This is particularly true for components that are laminated inside sandwich panels. Components that are faulty and/or fail during testing are much more difficult to remove and replace when incorporated into a MFS.

The later design faults and faulty components are spotted the more costly they are to rectify. The increase in this cost due to MFS will require that the quality control procedures used are more rigorous to ensure design faults are identified before a significant cost is incurred in their correction. This will slow down the process and require extra resources.

2.3. Multifunctional Solar Array Structure

Examples of the various forms of multifunctional structures (MFS) can be found in [4] which reviews the use of multifunctional structures for integrated electronics, harness, thermal management, embedded sensors and goes into detail on power storage and [5] where multifunctional structures are reviewed along with several other new spacecraft technologies.

The literature shows that a majority of the physical components of a spacecraft can be adapted to perform structural functions, that the structure of a spacecraft can be adapted to perform other subsystem functions and that new technologies can be brought together to create a multifunctional component.

Excluding the propulsion system and the spacecraft's structure, the electrical power system has the most mass (19% of the dry mass [6] and takes up considerable volume on the average spacecraft. The main functions of the electrical power system are power generation (solar array), power management (power conditioning and distribution unit (PCDU)), power storage (batteries) and power distribution (wiring harness).

By using new lower mass technologies and combining the functions together into a single structure the efficiency of the spacecraft is improved. The use of lighter components will reduce the mass of the spacecraft. The removal of the batteries and PCDU from inside the spacecraft reduces the internal volume requirement of the spacecraft and removes the parasitic structure associated with them. Placing the solar cells, batteries and PCDU in close proximity reduces the harness requirement.

This MFS is demonstrated in the ITN Energy Systems Flexible Integrated Power Pack (FIPP) [7]. The FIPP also indicates why such an MFS is yet to be used on a spacecraft. The FIPP has a thickness of at most a few millimetres and a very low density. As such it has very little thermal inertia and, since it is designed to be exposed to the sun, it will heat up and cool down very quickly. The temperatures experienced by the FIPP will exceed the operating limits of the components parts, particularly the batteries. This is true for all batteries, including those discussed in [4], particularly if the MFS is mounted as an external array rather than attached to the main body of the spacecraft where it can be supported by the spacecraft's greater thermal inertia and thermal control system.

As such, there would be a great benefit to the astronautics community if a thermal control solution were found that would allow a power generation and storage multifunctional deployed solar array. The purpose of this paper is to clarify the problem and highlight a possible way forward towards the solution of this issue.

3. DESCRIPTION OF MODEL

To determine the boundaries of the problem in terms of a steady state temperature that could be reached, a model was created using ThermXL. The model is a cell that would be used to create a much larger array, FIG 1. It is composed of a sandwich structure of CFRP facesheet and aluminium 5052 honeycomb core. GaAs solar cells are mounted on the lit side and a white paint coating on the dark side. A thin film battery, Varta PoLiFlex® PLF263441 D, is mounted in the centre of the cell. This model is identified as model 1.

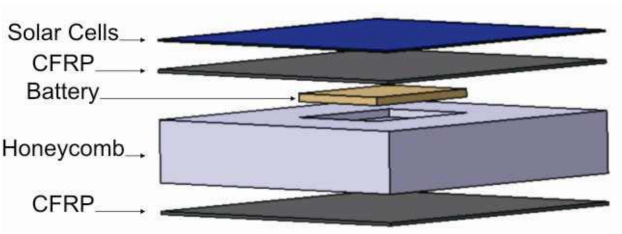

FIG 1. An exploded view of model 1, the baseline design.

This creates a model using readily available components which is thus a good representative of the most basic MFS. It builds on previous work [8][9] which looked at the structural properties of a very similar arrangement. The distance of the battery from the space facing side is varied to determine if there is a location inside the cell for the battery and thus no thermal control solution is required. The model is initially run in the steady state situation.

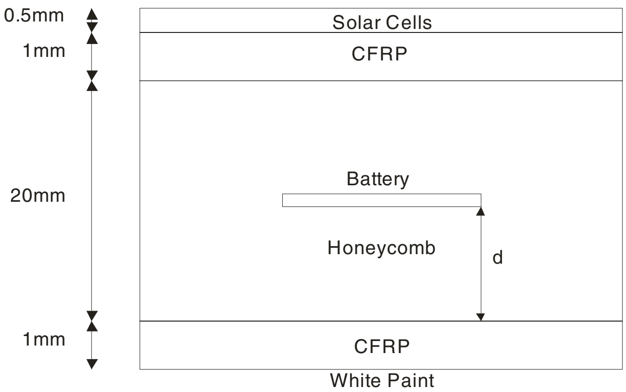

FIG 2. ThermXL model showing the composition of a section of a multifunctional solar array and the distance, *d*.

The model is 10cm by 10cm. The CFRP facesheets are 1mm thick. The honeycomb is 20mm thick. The solar cells including cover glass and substrate are 0.5mm thick.

The battery is 41mm by 34mm by 2.6mm thick. The battery is placed at the centre of the cell. The distance of the battery from the dark plate is indicated by *d,* FIG 2. The geometry is modelled as seven nodes placed at component boundaries with prescribed heat paths between them, FIG 3. Two heat paths through the model to the cold side are considered, one through the battery and its supports (Nodes 3, 4, 5 and 6) and one through the honeycomb (nodes 3 and 6), FIG 3. Nodes 1 and 7 are connected by a radiative link to an extra node, which represents cold space and is not shown, to model the heat output of the cell.

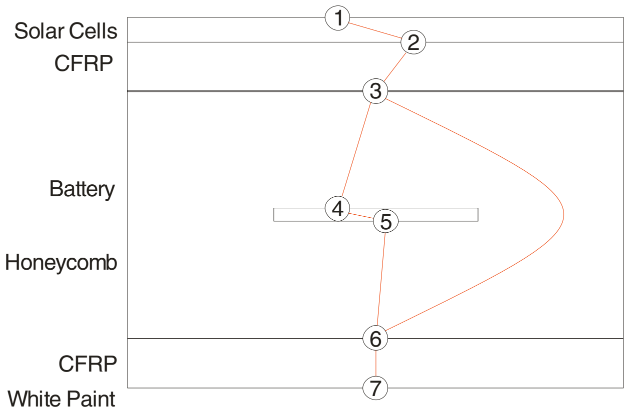

FIG 3. ThermXL model showing the heat paths through the multifunctional solar array. The nodes are offset for illustrative purposes only.

3.1.1. Model Variations

Three variations on model 1 are considered. In these models the battery is placed 0.008m from the dark side. These variations are possible solutions to the thermal problem that are simple and will show how the use of insulation affects the temperature of the battery and the array cell.

- Model 1a has carbon aerogel as an insulator on either side of the battery.
- Model 1b has carbon aerogel between the battery and the lit facesheet.
- Model 1c has carbon aerogel between the battery and the dark facesheet.

3.1.2. Environments

The models are exposed to two environments. The first environment places the cell between the sun and the earth. The second places the cell behind the earth in eclipse. A geosynchronous orbit is used as suitable example orbit. FIG 4 shows the positions of the two environments.

3.1.2.1. Environment 1 (Sun Lit) Inputs

The model is placed on the sun-earth vector between the sun and the earth and is orientated perpendicular to the vector. The solar cells are illuminated by the sun and the coated side is illuminated by the earth's albedo and infra red radiation. The battery is charging.

- Sun input of 1371 W/m^2 on node 1.
- Earth Albedo input of 14.4 W/m^2 on node 7.
- Earth infra-red of 5.6 W/m^2 on node 7.
- Battery charging heat output 0.11W shared equally between nodes 4 and 5.

3.1.2.2. Environment 2 (Eclipse) Inputs

The model is placed on the sun-earth vector and is orientated perpendicular to the vector. The sun is eclipsed by the earth. There is no sun or earth albedo input. The earth's infra red radiation illuminates the solar cells. The battery is discharging.

- Earth infra-red of 5.6 W/m^2 on node 1.
- Battery discharging heat output 0.007W shared equally between nodes 4 and 5.

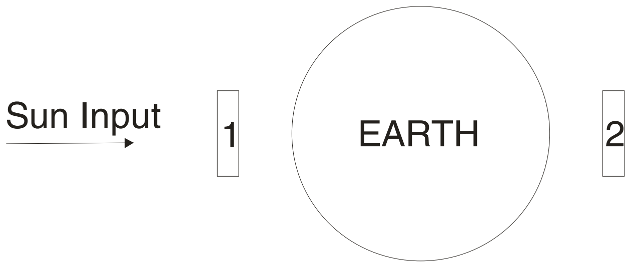

FIG 4. Diagram of the location of the two environments.

3.2. Model Assumptions

In order to simplify the mathematical model the following assumptions have been made:

- The cell is always perpendicular to any input. As such any inputs not perpendicular are considered to be zero.
- The earth emitted IR radiation is of a similar frequency to the IR radiation emitted by the surface. Thus the IR emittance value for the plate can be used as the absorption coefficient for the earth infra red radiation.
- The internal radiation of heat inside the honeycomb panels is negligible when compared to the conductive heat flow and is thus not considered to improve the simplicity of the model and remove sources of small numbers that would hinder convergence of the solution.
- A solar cell packing efficiency of 100% is assumed to simplify the model.
- There is no heat flow across the edges of the panel. There is also no heat flow across the heat paths identified in FIG 2.

3.2.1. Honeycomb Model

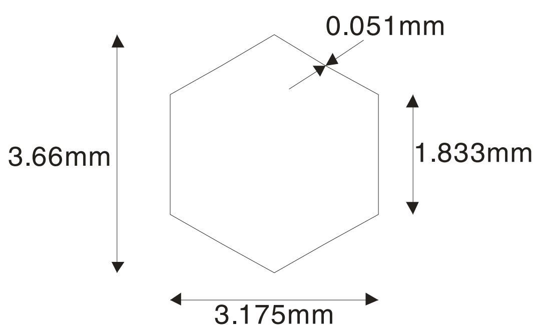

FIG 5. The geometry of a single cell of the honeycomb core used.

The honeycomb core will be modelled as a conductive link where the area available for conduction is determined by the percentage of the facesheet area that is in contact with the honeycomb material. For the geometry shown in FIG 5 this area is 5% of the area covered by the honeycomb.

3.3. Model Properties

The following are used to build the model.

- Solar cell thermal conduction = 160 W/mK.
- CFRP conduction = 110 W/mK [10].
- Carbon aerogel conduction = 0.04 W/mK [10].
- Honeycomb material conduction = 138 W/mK [10].
- Incoming sun flux = 1371 W/m^2.
- Incoming earth albedo = 14.4 W/m^2.
- Incoming earth infra-red = 5.6 W/m^^{2}.
- Solar cell optical properties: aborbtivity = 0.88, emittance = 0.8 [6].
- White paint optical properties: aborbtivity = 0.12, emittance = 0.9 [6].
- Varta PoLiFlex® operating temperatures: charge 273K to 318K, discharge 253K to 333K. [11]
- Lithium polymer battery conduction = 0.18 W/mK [12]
- Lithium polymer battery heat generation during charge = 30000W/m^3 [12].
- Lithium polymer battery heat generation during discharge = 5200W/m^3 [12].

4. RESULTS

4.1. Model 1: The Baseline

Two plots for each environment are presented. FIG 6 and FIG 8 plot the distance of the battery from the dark plate against the temperature of model nodes. Each series represents a node of the model. FIG 7 and FIG 9 show the temperature variation across the battery. Each series represents a different value of *d*.

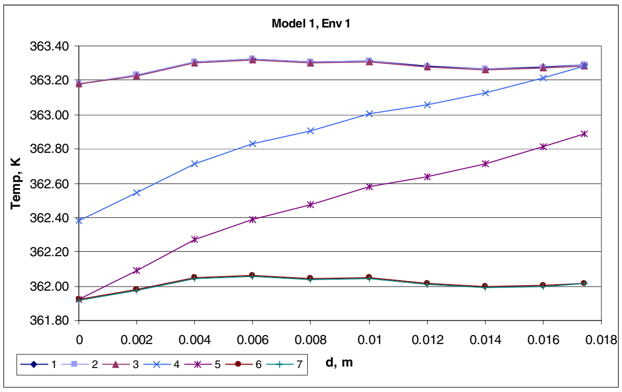

FIG 6. Model 1, Sun Lit, showing node temperature as a function of the battery location.

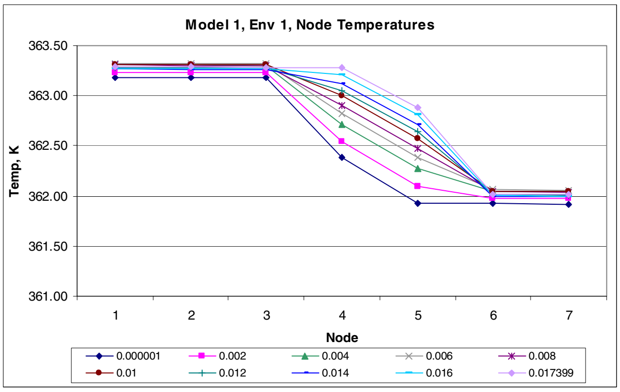

FIG 7. Model 1, Sun Lit, showing the variation of node temperatures across the array cell for each location of the battery.

In the sun lit environment, model 1 shows a limited temperature difference between two faces of the array, FIG 6. As the battery is moved towards the lit face (node 1) the temperature increases in a linear fashion. FIG 7 shows that the temperatures of the external faces do not vary with the location of the battery and that the rate of change of the temperature across the cell varies as the battery moves closer to the lit plate. When the battery is closer to the dark plate there is a more significant temperature step between nodes 3 and 4. When the battery is close to the lit side, this steep temperature change is now between nodes 5 and 6. This reflects the changing distances between these nodes as the battery moves closer to the lit side. The temperature change across the battery is constant.

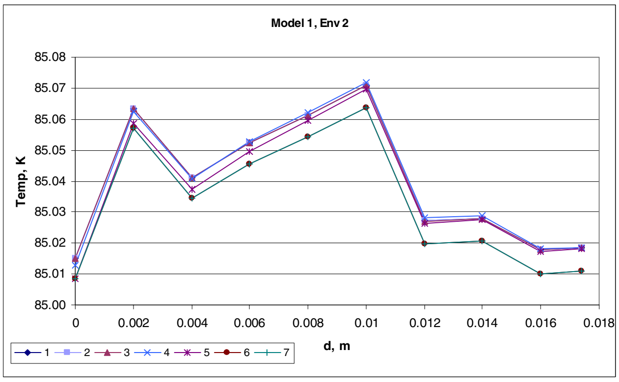

FIG 8. Model 1, Eclipse, showing node temperature as a function of the battery location.

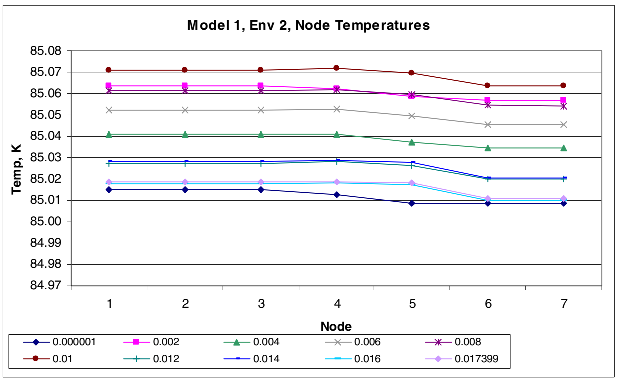

FIG 9. Model 1, Eclipse, showing the variation of node temperatures across the array cell for each location of the battery.

Model 1 environment 2 does not show a linear progression. The results are scattered across a very narrow temperature range, FIG 8 and FIG 9. The scatter is caused by the limits of the modelling software. The narrow temperature range indicates that the location of the battery has no effect on the temperature of the model.

4.2. Models 1a, 1b and 1c: The Insulation Models

FIG 10 shows the node temperatures for each model when in sun light, environment 1. FIG 11 shows the node temperatures for each model when in eclipse, environment 2.

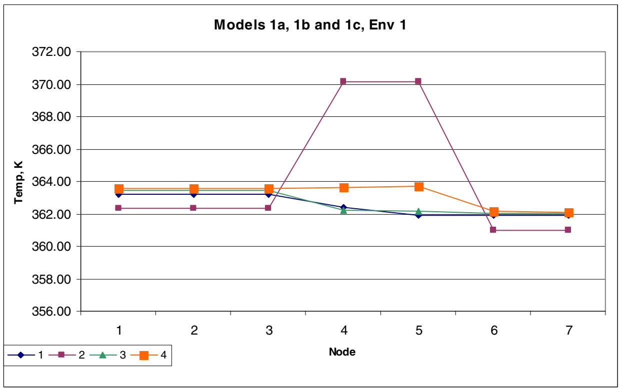

FIG 10. Node Temperatures of all the models in the sun lit environment.

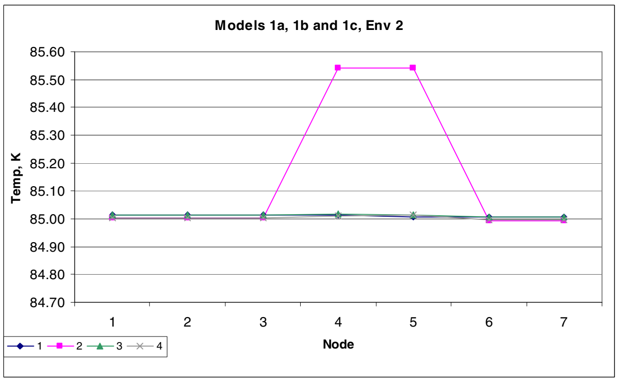

FIG 11. Node temperatures of all the models in the eclipse environment.

In model 1a, the presence of the insulation on both sides of the battery increases the temperature of the battery when sun lit and in eclipse. This is because the heat generated by the battery during charge and discharge is contained. The insulation in front of the battery in model 1b does not affect the temperature of the battery. It does alter the temperature distribution such that the temperature gradient across the cell occurs across the insulation rather than across the battery. Model 1c shows similar performance with the temperature change being solely across the insulation. In this case this occurs behind the battery, effectively raising the temperature of the battery. In the eclipse environment for all versions, the changes in temperature are negligible.

5. DISCUSSION

Model 1 shows that there is not a location in the array cell for a battery to be located that can maintain the battery within its specified temperatures. This is because the temperatures throughout the cell are too high in sun light and too low in eclipse with respect to the battery temperature limits. As such a thermal control solution is required to prevent the battery from over heating and freezing in a steady state model.

The use of insulation as a passive form of thermal control is not effective. Placing insulation on both sides of the battery raises the temperature of the battery, increasing the problem when sun lit. Insulation on only one side of the battery changes the temperature of the battery but only in that it alters which of the facesheet temperatures the battery matches. As such, the use of insulation on its own is not an effective solution for a steady state model.

The results indicate that the temperature difference across the array cell will have to be altered for a battery to be placed inside the array cell. A method of doing this would be to increase the surface area of the surfaces, by adding vanes, so that more heat is emitted in sun shine and more is collected in eclipse. However, only the dark side of the array is available as the solar cells cannot be disturbed. In the environments considered above increasing the surface area would add mass that would only help to cool the array. This is not a valid solution for all environments. Thus a steady state solution must be discounted and it will be necessary to add some active elements and perform transient analyses.

Further work will focus the use of transient analysis to determine if the rate of change of temperature of the solar array is such that the limits of the battery are not exceeded. The rate of change can be altered by the use of insulation, heaters, conductors and active control elements, for example shape memory alloys. The properties of the array structure and the components used will be selected to aid solution or minimise the problem. To this end experiments will be carried out to determine the thermal properties of these components.

6. CONCLUSION

Multifunctional spacecraft structures are an exciting and potentially very significant approach to spacecraft design. They will allow designers of spacecraft to minimise mass and volume and make spacecraft more efficient. This is particularly true for small satellites where budgets are tight and conventional configurations do not scale efficiently. A considerable saving can be offered by using the technology to place the batteries in the solar array. However the thermal tolerances of the components stop this technology from being used.

A model of a proposed multifunctional structure has been investigated in sun light and in eclipse and the steady state temperature determined. It was found that there was not a location in the array cell to place a battery as all temperatures of the cell are outside the limits of the battery. Three variations on the design involving insulation were modelled to determine if a steady state solution could be found. The insulation did not have a positive effect.

The results indicate that transient solutions should be investigated and possible methods of altering the conductivity and rate of change of temperature are suggested.

7. ACKNOWLEDMENTS

Alstrom Power Aerospace, Mechanical Engineering Services for the use of a trial ThermXL license.

8. REFERENCES

[1] Rossoni P. and Panetta P.V.; Developments in Nano-Satellite Structural Subsystem Design at NASA-GSFC. *Proceedings of the 13th AIAA/USU Conference on Small Satellites*. NASA, 1999.
[2] Jackson B. and Epstein K.; A Reconfigurable Multifunctional Architecture Approach for Next-Generation Nanosatellite Design. Volume 7 of *Aerospace Conference Proceedings*, pages 185-193. IEEE, March 2000.
[3] Bandecchi M., Melton B., and Ongaro F.; Concurrent engineering applied to space mission assessment and design. Technical Report ESABD8, ESA, September 1999.
[4] Aglietti G.S., Schwingshackl C.W., and Roberts S.C.; Multifunctional Structure Technologies for Satellite Applications. *Journal of Intelligent Material Systems and Structures*, 2007.
[5] Das A. and Obal M.W. Revolutionary Satellite Structural Systems Technology - a Vision for the Future. Volume 2 of *1998 IEEE Aerospace Conference*, pages 57-67. IEEE, 1998.
[6] Fortescue P.W., Stark J.P.W., and Swinerd G.G. Spacecraft Systems Engineering. Wiley, 3rd edition, 2003.
[7] Clark C., Summers J., and Armstrong J. Innovative Flexible Lightweight Thin-Film Power Generation and Storage for Space Applications. Volume 1 of *Proceedings of the Intersociety Energy Conversion Engineering Conference*, pages 692-698. IEEE, 2000.
[8] Roberts S.C. and Aglietti G.S. Battery performance degradation under vibration loading. DCSSS07, 2006.
[9] Roberts S.C. and Aglietti G.S. Multifunctional power structures for spacecraft application. *The Proceedings of the 57th International Astronautical Congress*, 2007.
[10] Automation Creations, Inc; *Matweb*. www.matweb.com.
[11] Varta; Varta PoLiFlex Data Sheets; http://www.varta-microbattery.com/en/oempages/varta_poliflex/varta_poliflex_en.php
[12] Chen Y. and Evans J.W. Three-Dimensional Thermal Modelling of Lithium-Polymer Batteries Under Galvanostatic Discharge and Dynamic Power Profile. Volume 141, Issue 11 of *Journal of the Electrochemical Society*, pages 2947-2955, November 1994.